



## MRI based genomic analysis of glioma using three pathway deep convolutional neural network for IDH classification

Sonal GORE<sup>1,2</sup>, Jayant JAGTAP<sup>3,\*</sup>

<sup>1</sup>Symbiosis International (Deemed University) (SIU), Pune, Maharashtra, India

<sup>2</sup>Pimpri Chinchwad College of Engineering, Pune, Maharashtra, India

<sup>3</sup>Symbiosis Institute of Technology (SIT), Symbiosis International (Deemed University) (SIU), Pune, Maharashtra, India

Received: 26.04.2021

Accepted/Published Online: 09.08.2021

Final Version: 04.10.2021

**Abstract:** As per 2016 updates by World Health Organization (WHO) on cancer disease, gliomas are categorized and further treated based on genomic mutations. The imaging modalities support a complimentary but immediate noninvasive diagnosis of cancer based on genetic mutations. Our aim is to train a deep convolutional neural network for isocitrate dehydrogenase (IDH) genotyping of glioma by auto-extracting the most discriminative features from magnetic resonance imaging (MRI) volumes. MR imaging data of total 217 patients were obtained from The Cancer Imaging Archives (TCIA) of high and low-grade gliomas. A 3-pathway convolutional neural network was trained for IDH classification. The multipath neural network, consisting of one shallow and two deep neural network paths, is used to auto-extract the significant imaging features for successful IDH discrimination into IDH mutant and wild type. An accuracy of 93.67% and cross-entropy loss of 0.052 is achieved for IDH classification. The results of 3-pathway convolutional neural network (CNN) are better than the results achieved from individual paths of 3-pathway model. The results have demonstrated the multipath convolutional neural networks as state-of-the-art method with simple design to predict IDH genotypes in glioma with auto-extraction of radiogenomic features.

**Key words:** Glioma, magnetic resonance imaging, radiogenomic analysis, multipath convolutional neural network, isocitrate dehydrogenase

### 1. Introduction

Predictive markers based on genetic signatures have recently gained a lot of attention in glioma cancer analysis because of revised classification of gliomas by World Health Organization (WHO) in the year 2016. Among these biomarkers, isocitrate dehydrogenase (IDH) mutation is a valuable prognostic and diagnostic biomarker which helps to predict for severity of diffuse glioma. It has become apparent that the experimental heterogeneity is related with IDH genotypes and with different survival rates for IDH mutant and wild type patients. In clinical exercise, invasive biopsy needs to be performed to confirm the genetic profiles of cancerous tumor using immunohistopathology methods, which are time consuming and costlier. However, such validation based on tissue sampling can be challenging, as it is evident from report by The Cancer Genome Atlas (TCGA) that around 35% in vivo surgeries obtained adequate tissue samples to confirm the IDH class [1]. Recently, noninvasive prediction using magnetic resonance imaging (MRI) is proved as more helpful for initial diagnosis and immediate treatment planning for cancer patients [2, 3]. The various machine learning algorithms [4–6] or

\*Correspondence: jayant.jagtap@sitpune.edu.in

deep learning techniques [7, 8] have been applied to radiogenomic studies of glioma to predict genotypes and survival outcomes. Among these, deep learning methods have demonstrated outperforming results as compared to classical machine learning approaches.

Machine learning based methods use hand crafted features by designing a classical pipeline, with which features are manually extracted and then given to a classifier. For these methods, classifier is trained with an assumption that input attributes have an adequate discriminative strength, since the behavioural working of classifier is independent from nature of those attributes. Such methods are challenging with many traditional machine learning techniques because of heavy computation to extract large number of features. This may improve the performance of model, but with large space and time complexities by making those models deliberate to compute and expensive.

An alternate method is based on deep learning techniques used for extracting the task-adapted features. It learns highly complex features from original raw data hierarchically and it has been revealed to surpass at learning such feature hierarchies. Deep learning techniques have been extensively accepted for learning task adaptive features in tumor segmentation or classification applications and these have demonstrated the outstanding performances. Although these performances have been remarkable, additional work is required to make these methods to get fully adopted in the clinical practice. Various deep learning models have been evaluated using different neural networks like convolutional neural network (CNN), recurrent neural network (RNN), stacked auto-encoder, long short-term memory (LSTM) etc. The models using CNNs are proven as best methods to handle the MR imaging-based classification tasks [9]. With this motivation, our study present an effective multipath CNN model with simple design for IDH discrimination and it is evaluated here using performance metrics including accuracy and cross-entropy loss. The multiple cascaded hidden layers of convolutional neural network activate the intermediate neurons by applying the weights in overlapping regions within a visual field of specific size. Each layer of network converts the raw input data into more complex, abstract representations in hierarchic manner. The set of features with different representations can be individually caught with different sequential paths of multipath network and such multipath network can learn more comprehensive, elusive features than a sequential network with single path. Therefore, it is hypothesized that our trained 3-pathway CNN model can predict IDH mutation in glioma patients by combining features with different representations extracted from three different paths. The model utilizes the global (top-level with abstract details) features extracted from shallow path of network and local (low-level with tiny details) features extracted from deep path of the network. Such an effective and simple model will definitely facilitate an imminent clinical interpretability of glioma cancer, which is a major challenge in this field. The major contributions of our study are listed below.

- IDH mutational status of glioma is a significant predictive biomarker to understand the severity of tumor and to decide its therapy accordingly. We have developed a noninvasive predictive model for IDH subtyping of glioma into mutant and wild type.
- We have designed a simple but effective 3-pathway CNN-based deep neural network. It learns local details as well as large contextual information by analysing multimodal data of routine MRI sequences and it performs fusion of such details for better IDH discrimination.

## 2. Related work

Nowadays, the role of radiomics based image processing has gained more importance in the field of medical data analysis using variety of MR imaging techniques [10]. Machine learning based experiments are gen-

erally designed with typical workflow including feature extraction, feature reduction with selective features, supervised or unsupervised feature learning for classification or regression, evaluation of model [11]. Various supervised/unsupervised/clustering techniques such as naive Bayes classifier, support vector machine, artificial neural networks, random forests, linear regression, logistic regression, k-means clustering, nearest neighbors, etc. are used to investigate the underlying biology of brain tumors [12–15]. However, the machine learning based methods are time consuming due to handcrafting of features and those also need expert interventions. Besides, the deep learning techniques are capable of auto-learning the task-adapted features without the need of an external feature engineering.

Few current research works have gained an effective attention over deep learning methods to solve the problem of IDH genotyping of glioma. The fusion of multimodal MRI data with deep learning methods enhanced the performance accuracy of few diagnostic model designs. Now, deep learning has become advanced and powerful predictive analytics tool with autonomous self-learning capability [16]. Deep learning methods discover useful insight from input data attributes automatically in hierarchical manner from local to global representation. Such useful, auto-derived features are proved as very important for further prediction with classification or regression tasks [17]. Deep learning-based techniques mainly include convolutional neural networks, deep belief networks, recurrent neural networks, long short-term memory, etc. [18].

Unlike the majority of studies, Yogananda et al. used complex 3D dense UNET for simultaneous voxel-wise segmentation as well as IDH classification, and demonstrated the cross-validated accuracy of 97.11% using only T2-weighted (T2w) 3D patches. The patches of size 32x32x32 were trained and tested using three-fold cross validation to perform voxel-wise classification by providing label 1 to IDH mutated voxel and label 2 to IDH wild voxel. Finally the majority voting over the voxel-wise classified labels has decided the final IDH class for whole tumor volume [3]. The prediction of IDH genotype with 1p/19q loss and methylguanine-DNA methyltransferase (MGMT) promotor methylation in tumorigenesis was well measured with leveraged performance of deep convolutional neural networks. It has used principal component analysis approach to perform the selection of nonredundant and highly sensitive features extracted from last hidden layer [19]. The transfer learning approach to reuse pretrained deep neural networks was proved as a potential method to perform MRI image analysis for glioma grading assessment. The feature analysis, learnt from large, colored, natural ImageNet dataset, has reliably predicted glioma grading when already inferred feature knowledge was shifted to small, gray, MRI image dataset for analysis [20]. The predictive performance of 34-layered residual network was cross-validated with three different network designs. It includes single combined network design using multiplane multimodal MR input, separate network design using plane wise MRI and separate network design using modality wise MRI data. The result of deep learning model with combined modality network design yielded an accuracy of 85.7% during testing, which was enhanced up to 89.1% with age as an additional contributory marker [21]. There are more chances of overfitting of deep neural network with small data due to high predictive capacity of model. But data augmentation techniques aid to increase the size of samples to avoid overfitting. The multiscale CNN used in the study by [22] is a 5-pathway model with different convolutional kernel sizes, which finally combines 5 output feature vectors in final layers of CNN. This model evaluated overfitted results with small database without data augmentation, but performed accurately with 30-fold augmented data. In the study by [23] high responsive filters are selected from last layer of CNN to extract the appropriate distinctive features and such deep CNN sufficiently discriminated IDH based glioma types. The effectiveness of deep learning architectures with 3D models was enhanced to classify IDH genotype dealing with 3D multimodal medical images and the transfer learning technique further evaluated an improved

generalizability of such model to predict the conventional histological grading [24]. A very deep design of CNN model (ResNet) with the residual learning using skip connections solved an issue of performance degradation, which occurred due to the problem of vanishing gradients [25]. The high recognition accuracy is yielded using residual CNN, which operated directly on whole 2D images of glioma without any need of segmentation task to extract the region of interest (ROI) [26]. Such residual network design improved the performance for IDH prediction as well as it provided detailed insight to discriminate tumor molecular class by exploring internal working of CNN and looking at the activation map of higher layer of network. Similar work is presented to highlight the use of activation maps, which experimented to know the features learnt by intermediate layers of CNN and captured more interpretability of the model, instead of using it as a black box [27]. Recently, an impact of motion corruption on IDH categorization is evaluated and an improvement is demonstrated by the motion-corrected deep model by Nalawade et al. [28]. The model designed by Pasquini et al. is a network specifically for glioblastoma cancer to categorize IDH-based classes. Their 2D CNN architecture was made up from four convolutional blocks containing total 7 convolution layers sequentially, which are further followed by two dense layers and softmax layer to generate two-class probability map. It produced highest performance for T1-weighted (T1w) and fluid attenuated inversion recovery (FLAIR) MRI sequences with almost same accuracy of 77% for both the MR modalities [29]. Few models have performed genomic classification of glioma by using the combined set of hand-engineered features and auto-extracted features, which are learnt by intermediate convolution layers of deep networks. The presence of combined mutations of IDH and TERT promoter is predicted by designing a support vector machine based model and this has used combined set of features: texture features extracted from fifth convolution layer of pretrained AlexNet and conventional radiomic features [30]. The multitask learning is carried out for simultaneous prediction of histological grade, IDH mutational status and 1p/19q codeletion status of glioma tumor using CNN-based pipeline and it yielded classification AUC of 0.94, 0.86 and 0.87 on independent test dataset for grade, IDH, 1p/19q status, respectively [31]. The studies related to cancer biology found that IDH mutant type of glioma exhibits less aggressive carcinogenesis process, related to glioma formation and further growth, as compared to more aggressive behaviour by IDH wild type [32, 33]. It is also found by few studies about better survival rate for IDH mutant class as compared with IDH wild type and these have used deep CNN models for survival prediction [34, 35]. In this study, we employ simple, but an improved model that can detect elusive differences between IDH classes to support an accurate discrimination of IDH genotype. Our deep neural network-based work proposes multipath convolutional neural network with the capability to auto-discriminate IDH types of glioma. We, therefore, evaluate a 3-pathway CNN model for the molecular classification of high-grade glioma (HGG) and low-grade glioma (LGG).

Although there are few recent studies either using deep learning model [3] or radiomic model [36] which have demonstrated higher accuracy or specificity. These existing models are either complex with a greater number of neural network layers (majorly fully connected) or these have used rare, costly MRI modality like diffusion or perfusion weighted MRI. But the proposed deep learning-based model has come with simple multipath network design with hardly maximum 13 convolution layers and with 4-sequence MRI data, which is obtained using widely available, routinely performed MRI modalities.

### 3. Material and method

#### 3.1. Data preparation

MR imaging data and its corresponding genomic details were fetched from the publicly available database: The Cancer Imaging Archive and The Cancer Genome Atlas [37, 38]. Only the presurgical volumes of four

MRI modalities including T1-weighted, T1-weighted with contrast enhanced (T1ce), T2-weighted and fluid attenuated inversion recovery were used in the study. The dataset consisted of 217 patients of high-grade glioma and low-grade glioma including 97 IDH mutant and 120 IDH wild type. The four modal MRI dataset of 217 patients contain total 768 volumes of size  $200 \times 200 \times 40$ . Each original MRI volume, which is downloaded from TCIA website, is of size  $240 \times 240 \times 155$ . The 3D patch, consisting of 40 consecutive slices, is extracted from original 3D volume containing maximum tumor region. This patch extraction is automated using python implementations. Each tumor comprises three different regions namely enhancing tumor, nonenhancing tumor or necrosis region and region of edema. The attributes of each region varies as per IDH mutational status. Further, the preprocessing was applied by performing N4 bias field correction [39] to eliminate the in-homogeneity, and by performing normalization of image intensities to zero mean and unit variance [40].

### 3.2. Method

A model with three path CNN approach is defined here for IDH classification task. The proposed methodology used the CNN architecture as shown in Figure 1.

3D volumes, each of size  $240 \times 240 \times 40$ , taken from four MRI modalities are provided as an input to the model. Every scan was preprocessed to be zero mean and unit variance. The multiple paths help to acquire the local as well as global level features and thus help the neural network to learn more effectively. This type of architecture is good for such applications having sparse labels. The three pathways are decided considering small, medium, large receptive field sizes in order to estimate global and local dependencies of neighbouring pixels. Path-1 has more focused on extraction of global-level contextual information and path-2, path-3 have coarse-grained the local dependency of neighbourhood regions. Finally, the impact of different receptive field sizes was fused by concatenating the output of last layer of every path in the next step. The number of parameters for our model is 179, 963, and 416. The parameters used in layers of individual path and complete pathway are shown in Table 1.

The suitable network layout and internal design is decided by using random formations and parameter tuning method. The hyperparameter selection is performed intuitively with random search. Selection through random search is faster than grid search method and human intuition is still helpful in this case. The hyperparameter tuning is done using HyperModel instances of Keras Tuner library. The parameters such as dropout rate, number of activation kernels in the convolutional layer, activation function type, number of neurons for dense layer are optimized by specifying the maximum, minimum, default or range values. Such prior knowledge about every parameter is incorporated in the search space of Tuner. For example, to set for number of activation kernels, the range was provided from 64 to 512. The learning rate was also tweaked on a log scale by specifying the range values from  $1e-5$  to  $1e-2$ . The number of paths and number of convolutional layers in each path were decided with random configurations and the model was fit on subset of training samples to speed up the search process.

Detailed network design is as follows: The images of size  $200 \times 200 \times 40$  from four different MRI modalities is provided randomly to the input layer in the batches of eight images. In path-1, the activation kernels of size  $13 \times 13$  and  $9 \times 9$  are applied to perform convolution on input images in two consecutive convolutional layers with no padding and rectified linear unit (ReLU) activation function at each layer. The second layer is followed by  $2 \times 2$  max-pooling and dropout layer with removal of 30% of vanishing gradients. The dropout layer is placed to avoid the problem of overfitting. The number of activation filters used are 64 in both convolutional layers of path-1. The output size of image after 2nd layer is  $43 \times 43 \times 128$ . This path-1 helps to extract the high-level features by making use of filters with bigger size. Then, in path-2, from first to fourth convolutional layer, the

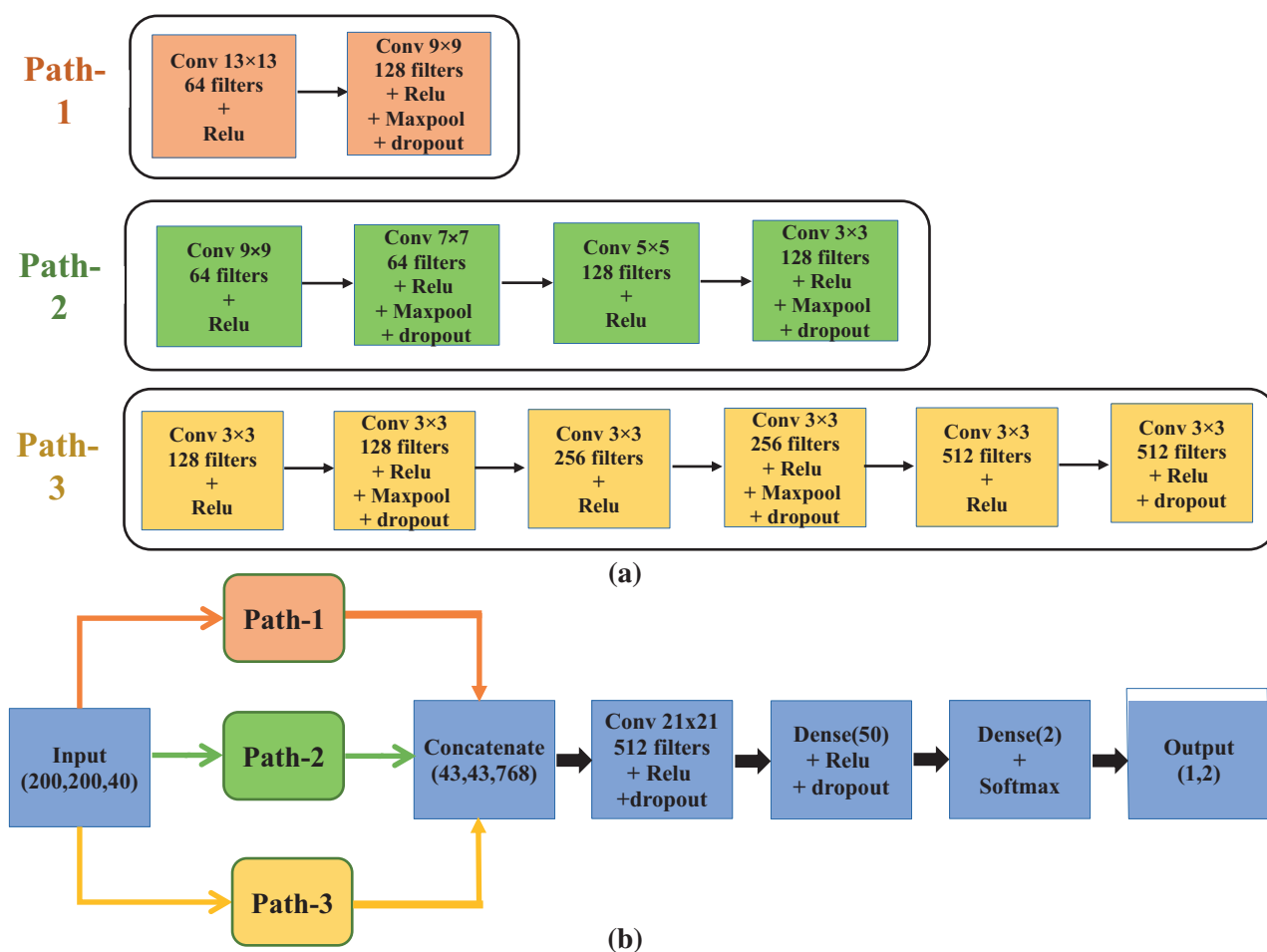


**Figure 1.** Architecture of three pathway convolutional neural network. (a) It shows the architecture of convolutional layers used in three different paths, namely, path-1, path-2, and path-3. Each convolution block presents the details of elements used at any particular layer. The details are such as size of activation filters, number of filters, activation function name, pooling layer, dropout layer. (b) It shows the architecture of complete 3-pathway CNN. It represents the concatenation layer, followed by convolution layer and dense layers to provide binary classification output.

number of activation filters used are 64, 64, 128, 128. These filters used in four layers are of size  $9 \times 9$ ,  $7 \times 7$ ,  $5 \times 5$  and  $3 \times 3$  respectively. After every two convolutional layers, maximum pooling of size  $2 \times 2$  is applied, which is followed by dropout layer to avoid the overfitted learning of network. The fourth convolution layer of path-2 has generated output of size  $43 \times 43 \times 128$ . Further, with path-3, an activation maps are generated by applying the convolutional filters of size  $3 \times 3$  in six consecutive convolutional layers by using 128, 128, 256, 256, 512, 512 number of filters successively. The max-pooling of size  $2 \times 2$  is applied at second and fourth convolution layers, which is followed by dropout layer with dropout rate of 25% and 30%, respectively. The sixth convolution layer is simply followed by dropout layer with rate of 40% and it produced an output of size  $43 \times 43 \times 512$ . The path-2 and path-3, with its complex and deep design, helps to capture the low-level features by understanding the local regions differently in better ways. Furthermore, the feature vectors of size 128, 128, 512 generated at the end of path-1, path-2, path-3 are combined together to create a large feature vector comprising total 768 local as well as global features. The merged feature map from all three convolution paths is connected to

**Table 1.** Summary of parameters used in layers of individual path and complete 3-pathway model.

Parameters	Path-1	Path-2	Path-3	Complete 3-pathway model
Number of convolution layers	2	4	6	13
Names of layers	1st and 2nd layers	1st, 2nd, 3rd, and 4th layers	1st, 2nd, 3rd ,4th, 5th, and 6th layers	13th layer after merging three paths
Number of activation kernels used	64 in 1st and 2nd layer	64 in 1st and 2nd layer, 128 in 3rd and 4th layer	128 in 1st and 2nd layer, 256 in 3rd and 4th layer, 512 in 5th and 6th layer	Total 2816 kernels: 2304 in three individual paths + 512 in 13th convolution layer
Size of activation kernels	13×13 and 9×9	9×9, 7×7, 5×5 and 3×3	3×3	21×21 in 13th layer
Activation function used	ReLu in each layer	ReLu in each layer	ReLu in each layer	ReLu in all 13 convolution layers
Pooling type used and its size	Maximum pooling with 2 x 2 size in 2nd layer	Maximum pooling with 2 x 2 size in 2nd and 4th layers	Maximum pooling with 2 x 2 size in 2nd and 4th layers	Total 5 pooling layers of three individual paths
Dropout rates used	30% in 2nd layer	25% in 2nd layer and 30% in 4th layer	25% in 2nd layer, 30% in 4th layer and 40% in 6th layer	25%, 30%, 40% in three individual paths and 50% in 1st dense layer
Number of dense layers	–	–	–	2
Number of neurons in dense layers	–	–	–	50 neurons in first layer and 2 neurons in second layer

one more convolution layer designed with 512 activation kernels of size  $21 \times 21$ , which is followed by dropout layer with 50% dropout rate. Finally, the output of this convolution layer is inputted to first fully connected (dense) layer with 50 neurons. Such flattened output is fed as an input to final dense layer with two neurons to generate the probabilities for two classes as IDH mutant and IDH wild type. ReLu activation function is used in all 13 convolution layers and one dense layer. And the softmax activation function is used with final dense layer to generate two-class classification output. The model hyperparameters are selected after careful tuning of network empirically. The weights for all layers are initialized using zero mean normal distribution initializer with standard deviation of value 0.01 and the biases are initialized with zero value. The adaptive moment estimation (Adam) optimizer is used with learning rate of value 0.00001.

An average classification accuracy was used to measure classification results and used the categorical cross-entropy to calculate the network error loss. The dataset is partitioned into three subsets using train-test split during experimentation: 60% data for training, 20% for validation and 20% for test. Python and

Keras library with TensorFlow backend was used for the experimentation. The experimentation was conducted using 64-bit Windows10 operating system on Intel core i5 9th generation machine with single NVIDIA 4GB GEFORCE GTX 1650 GPU.

#### 4. Results

The proposed 3-pathway architecture achieved f1-score of 92.19%, precision value of 97.01%, recall value of 87.83%, validation accuracy of 94.25% and test accuracy of 93.67%. Whereas an individual paths employed the validation accuracy, which is dropped down to 78.73% and achieved test accuracy up to 81.03%. The highest accuracy up to 99.78% are obtained with training phase during experimentation. The results of 3-pathway CNN model along with the results obtained for each individual path of 3-pathway model are shown in Tables 2 and 3. Accuracy values obtained during training, validation and testing phase are tabulated in Table 2.

**Table 2.** Accuracy attained during training, validation and testing phase.

Model	Training accuracy(%)	Validation accuracy(%)	Testing accuracy(%)
Path-1 of 3-pathway model	93.26	78.73	81.03
Path-2 of 3-pathway model	94.42	87.35	89.08
Path-3 of 3-pathway model	94.42	87.35	87.93
3-pathway CNN model	99.78	94.25	93.67

Table 3 has shown the cross-entropy loss obtained during training, validation and testing phase for 3-pathway model as well as for every individual path of 3-pathway model. The 3-pathway model has achieved loss of 0.052 while testing the performance of model with separate patient cohort of 174 subjects.

**Table 3.** Cross-entropy loss attained during training, validation and testing phase.

Model	Training loss	Validation loss	Testing loss
Path-1 of 3-pathway model	0.070	0.180	0.164
Path-2 of 3-pathway model	0.055	0.119	0.114
Path-3 of 3-pathway model	0.056	0.120	0.119
3-pathway CNN model	0.002	0.051	0.052

The confusion matrix of 3-pathway model is shown in Figure 2.

Since the global or upper level features (abstract representation) extracted with shallow network (path-1) and local or low level features (fine-detailed representation) extracted with deeper network (path-2 and path-3) are combined together in 3-pathway model. Therefore, it can be observed from the table that the 3-pathway architecture has achieved better results as compared to individual path's performance for accuracy as well as for loss values. The graphs for all performance measures calculated for our 3-pathway model are shown in Figure 3.

The intermediate feature maps generated by an individual path of 3-pathway CNN for one sample test subject of IDH wild type are visualized using Keras library and are shown in Figure 4.

It can be seen that as network goes more deeper from path-1 to path-3, the more detailed and abstract information is represented by path-3 as compared to other two paths. It is also observed that few activation filters have not learnt anything during training. Therefore, visualization of such activation maps is blank in



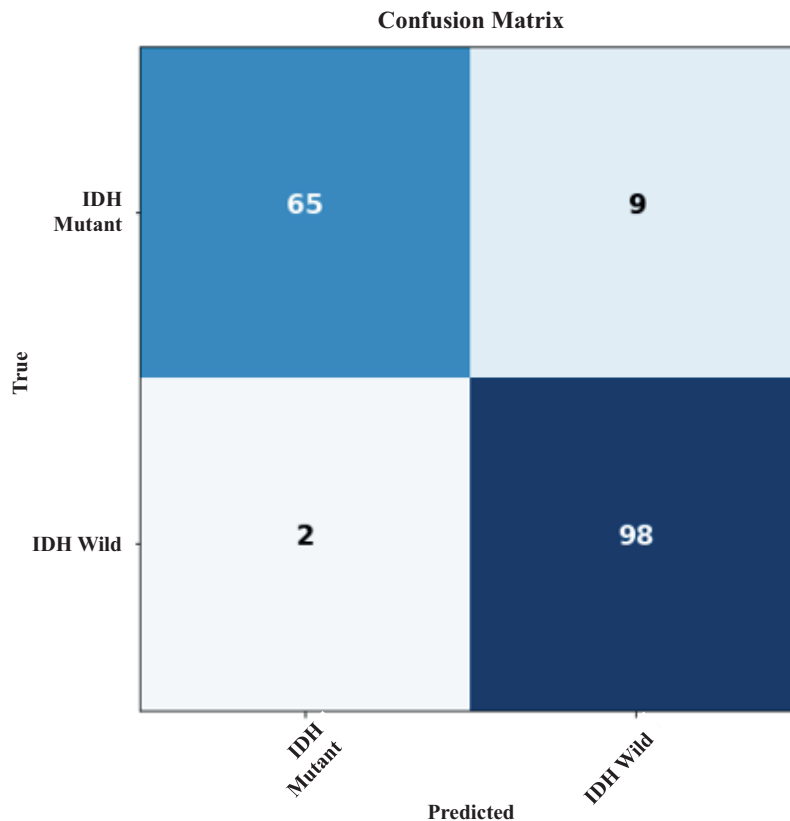


**Figure 2.** Confusion matrix of 3-pathway model. It shows the number of actual labels on Y-axis and the number of predicted labels on X-axis for IDH mutant and IDH wild type.

Figure 2. It is also seen that majority of IDH wild type tumors encompasses edema region in addition to enhancing core area, whereas majority of IDH mutant tumors involves the enhancing core region.

The performance of 3-pathway CNN is compared with existing state-of-the-art methods as shown in Table 4, where all models are evaluated for IDH binary classification.

The comparison is done with respect to various criteria like model performance, dataset and its size, MRI modalities, methodology. It can be observed that the 3-pathway CNN model achieved improved performance as compared with existing methods. It can also be observed that the proposed model carries simple design as compared to existing models in terms of number of convolutional layers. This leads to less run-time complexities. Also the use of multiparametric data, which is obtained from routine MRI sequences, extends the generalizability of model by making it more robust. Moreover, the inclusion of high-grade as well as low-grade glioma expands the capacity of model to encompass heterogeneous tumor samples in clinical translation of cancer. In addition, the 3-pathway model is experimented on variety public datasets for analysis of three different biomedical applications. Its details are specified in supplementary material. The results obtained on different datasets are provided in Tables S1 and S2. The accuracy and loss graphs are presented in Figures S1 and S2.

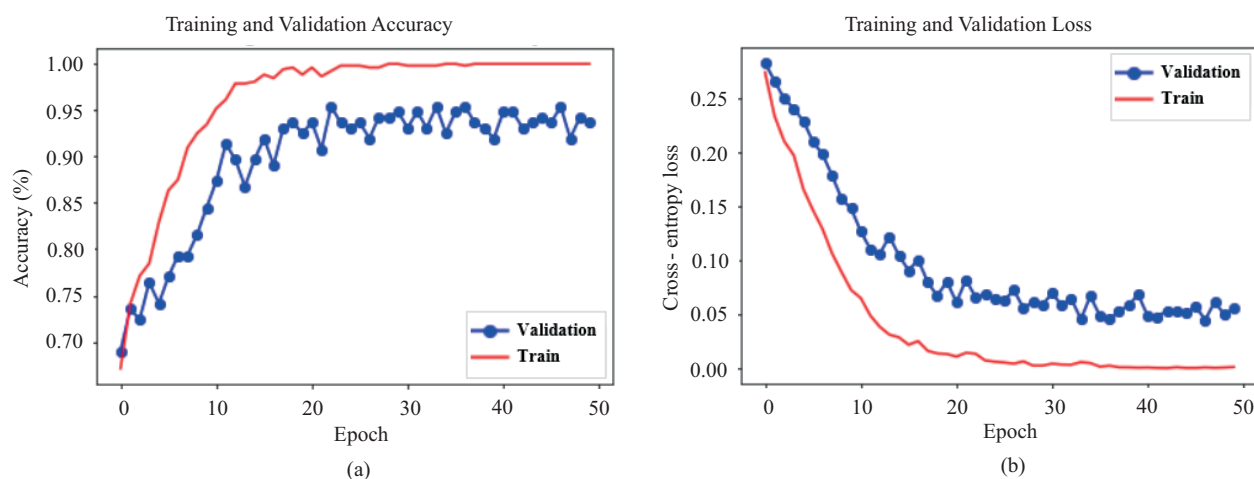


**Figure 3.** Graphs of accuracy and cross-entropy loss obtained during training and validation. (a) It shows the graph for accuracy obtained during training and validation phase of 3-pathway CNN model. (b) It shows the graph for cross-entropy loss obtained during training and validation phase of 3-pathway CNN model. The number of epochs is shown on x-axis and the related performance measure value is shown on y-axis.

**Table 4.** Comparison with existing methods.

Author, year	Accuracy (in %)	Precision, recall, f1-score (in %)	Loss function, loss value	Dataset used, MRI modalities used	Number of patients	Methodology
Nalawade et al. [2], 2019	83.8	84.1, 83.5, 83.5	-, -	The Cancer Imaging Archive (TCIA), MRI modalities: T2w	260	5-fold cross validation, 2D model with 161 densely connected convolution layers
Chang et al. [21], 2017	85.7	-, 79.1, -	Binary cross entropy, -	TCIA and local hospital, MRI modalities: T1w, T1ce, T2w, FLAIR	496	Train-validate-test split with 8:1:1 ratio, 34 convolution layers with residual connections
Ahmad et al. [26], 2019	86.7	93.54, 70.73, 80.55	Categorical cross entropy, -	Local hospital, MRI modalities: T2w	71	4-fold cross validation, 50 convolution layers with identity blocks for residual connections followed by one dense layer
Pasquini et al. [29], 2021	83	-, 76, -	Categorical cross entropy, 0.64	Local hospital, MRI modalities: T1w, T2w, FLAIR, rCBV, ADC	100	Glioblastoma-specific model design, 5-fold cross validation, 7 convolution layers followed by two dense layer, highest accuracy with rCBV MRI modality
3-pathway CNN (proposed method)	93.6	97.01, 87.83, 92.19	Categorical cross entropy, 0.052	TCIA, MRI modalities: T1w, T1ce, T2w, FLAIR	217	Train-validate-test split with 3:1:1 ratio, three pathway design with total 13 convolution layers followed by two dense layers

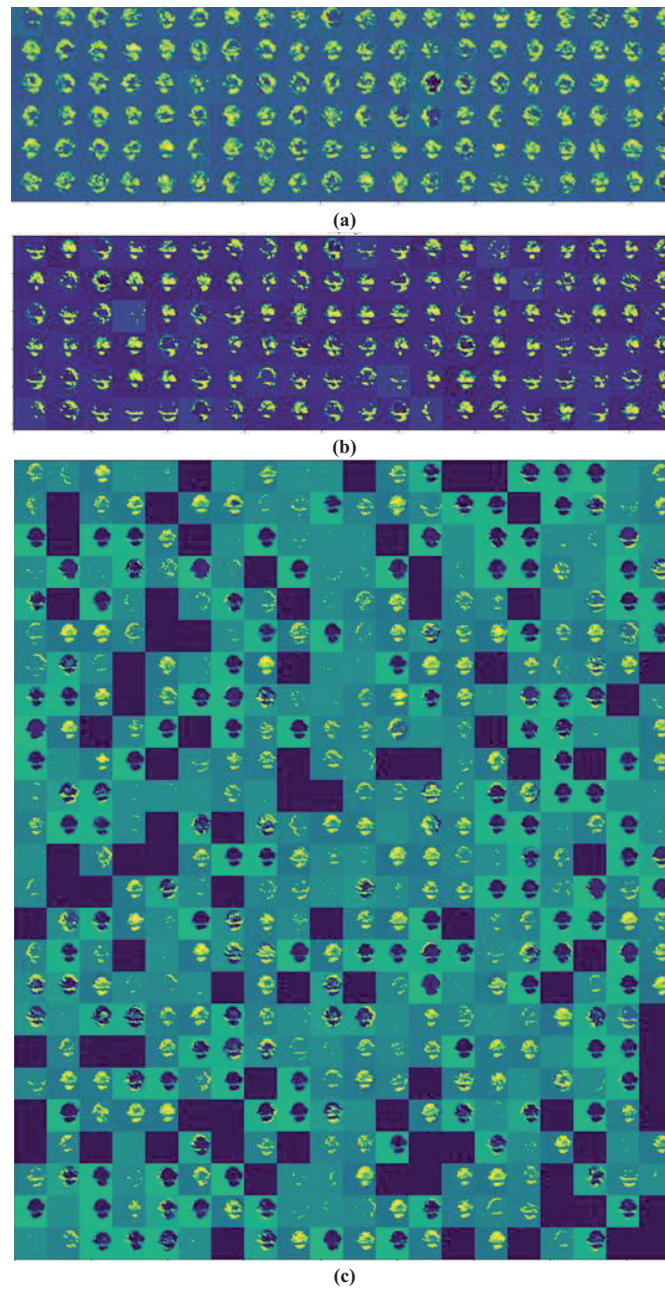


**Figure 4.** Activation maps of intermediate layers of 3-pathway CNN model. It shows intermediate activation maps generated by an individual path of 3-pathway CNN model i.e. path-1, path-2, and path-3. The activation maps of 20 images are visualized per row. (a) and (b) They show the visualization of feature map generated by last convolution layer of path-1 and path-2 with 128 activation kernels each. (c) It presents the visualization of feature map generated by last convolution layer of path-3 with 512 activation kernels.

## 5. Conclusion

An advanced research of convolutional neural network is conducted for MRI based IDH classification of glioma. The proposed 3-pathway network extracted more discriminate features than single path models. The model has successfully learnt the features taken from shallow as well as deep neural network paths and demonstrated the

performance improvement with an accuracy of 93.67% and error loss of 0.052 over the performance obtained with individual paths. Therefore, it can be concluded that multipath convolutional neural network shows more advantages than simple or single path networks. The model has a simple design and is capable of extracting wide series of features from simple to complex category, by understanding and representing the input in better way. In future, this model can be further enhanced to predict the survival rate of glioma patients based on such IDH based radiogenomic analysis.

### References

- [1] Cancer Genome Atlas Research Network. Comprehensive genomic characterization defines human glioblastoma genes and core pathways. *Nature* 2008; 455 (7216): 1061-1068.
- [2] Nalawade S, Murugesan G, Vejdani-Jahromi M, Fiscaro R, Yogananda C et al. Classification of brain tumor isocitrate dehydrogenase status using MRI and deep learning. *Journal of Medical Imaging* 2019; 6 (4): 1-13.
- [3] Yogananda CGB, Shah B, Vejdani-Jahromi M, Nalawade S, Murugesan G et al. A novel fully automated MRI-based deep-learning method for classification of IDH mutation status in brain gliomas. *Neuro-oncology* 2020; 22 (3): 402-411.
- [4] Zhang X, Tian Q, Wang L, Liu Y, Li B et al. Radiomics strategy for the molecular subtype stratification of lower-grade glioma: detecting IDH and TP53 mutations based on multimodal MRI. *Journal of Magnetic Resonance Imaging* 2018; 48 (4): 916-926.
- [5] Meraj T, Hassan A, Zahoor S, Rauf HT, Lali MI et al. Lungs nodule detection using semantic segmentation and classification with optimal features. *Preprints* 2019; 2019090139. doi: 10.20944/preprints201909.0139.v1
- [6] Korfiatis P, Kline TL, Coufalova L, Lachance DH, Parney IF et al. MRI texture features as biomarkers to predict MGMT methylation status in glioblastomas. *Medical Physics* 2016; 43 (6): 2835–2844.
- [7] Villanueva-Meyer JE, Wood MD, Choi BS, Mabray MC, Butowski NA et al. MRI features and IDH mutational status of grade II diffuse gliomas: impact on diagnosis and prognosis. *AJR American Journal of Roentgenology* 2018; 210 (3): 621-628.
- [8] Mossa A, Çevik U. Ensemble learning of multiview CNN models for survival time prediction of braintumor patients using multimodal MRI scans. *Turkish Journal of Electrical Engineering & Computer Science* 2021; 29: 616-631. doi: 10.3906/elk-2002-175
- [9] Zadeh Shirazi A, Fornaciari E, McDonnell MD, Yaghoobi M, Cevallos Y et al. The application of deep convolutional neural networks to brain cancer images: a survey. *Journal of Personalized Medicine* 2020; 10 (4): 224. doi: 10.3390/jpm10040224
- [10] Stefan B, Roland W. A Survey of MRI-based medical image analysis for brain tumor studies. *Physics in Medicine and Biology* 2013; 58 (13): R97-129.
- [11] Bastanlar Y, Ozuysal M. Introduction to machine learning. *Methods in Molecular Biology* 2014; 1107: 105-128.
- [12] Inza I, Calvo B, Armananzas R, Bengoetxea E, Larranaga P et al. Machine learning: an indispensable tool in bioinformatics. *Methods in Molecular Biology* 2010; 593: 25-48.
- [13] Zhang B, Chang K, Ramkissoon S, Tanguturi S, Bi WL et al. Multimodal MRI features predict isocitrate dehydrogenase genotype in high-grade gliomas. *Neuro-oncology* 2016; 19 (1): 109-117.
- [14] Dalu Y, Ganesh R. Evaluation of tumor-derived MRI-texture features for discrimination of molecular subtypes and prediction of 12-month survival status in glioblastoma. *Medical Physics* 2015; 42 (11): 6725-6735.
- [15] Songtao Q, Lei Y. Isocitrate dehydrogenase mutation is associated with tumor location and magnetic resonance imaging characteristics in astrocytic neoplasms. *Oncology Letters* 2014; 7: 1895-1902.

- [16] Bini S. Artificial intelligence, machine learning, deep learning, and cognitive computing: what do these terms mean and how will they impact health care? *The Journal of Arthroplasty* 2018; 33 (8): 2358-2361.
- [17] Ueda D, Shimazaki A, Miki Y. Technical and clinical overview of deep learning in radiology. *Japanese Journal of Radiology* 2019; 37: 15-33.
- [18] Xue Y, Chen S, Qin J, Liu Y, Huang B et al. Application of deep learning in automated analysis of molecular images in cancer: a survey. *Contrast Media Molecular Imaging* 2017; 9512370.
- [19] Chang P, Grinband XJ, Weinberg XBD. Deep-learning convolutional neural networks accurately classify genetic mutations in gliomas. *AJNR American Journal of Neuroradiology* 2018; 39: 1201-1207.
- [20] Yang Y, Yan LF, Zhang X. Glioma grading on conventional MR images: a deep learning study with transfer learning. *Frontiers in Neuroscience* 2018; 12 (804): 1-10.
- [21] Chang K, Bai HX, Zhou H, Chang S. Residual convolutional neural network for the determination of IDH status in low- and high-grade gliomas from MR imaging. *Clinical Cancer Research* 2017; OF1-OF9.
- [22] Akkus Z, Ali I, Sedlar J. Predicting 1p19q chromosomal deletion of low-grade gliomas from MR images using deep learning. *Journal of Digit Imaging* 2017; 30 (4): 469-476.
- [23] Li Z, Wang Y, Yu J, Guo Y, Cao W. Deep learning based radiomics (DLR) and its usage in non-invasive IDH1 prediction for low grade glioma. *Scientific Reports* 2017; 7: 5467.
- [24] Liang S, Zhang R, Liang D et al. Multimodal 3D DenseNet for IDH genotype prediction in gliomas. *Genes* 2018; 9 (8): 382.
- [25] He K, Xiangyu Z, Shaoqing R, Sun J. Deep residual learning for image recognition. In: *Proceedings of the IEEE conference on computer vision and pattern recognition; Las Vegas, US; 2016. pp. 770-778.*
- [26] Ahmad A, Sarkar S, Shah A, Gore S, Santosh V et al. Predictive and discriminative localization of IDH genotype in high grade gliomas using deep convolutional neural nets. In: *IEEE 16th International Symposium on Biomedical Imaging (ISBI); Venice, Italy; 2019. pp. 8-11.*
- [27] Chougule T, Shinde S, Santosh V, Saini J, Ingalthalika M. On Validating multimodal MRI based stratification of IDH genotype in high grade gliomas using CNNs and its comparison to radiomics. In: *International Workshop on Radiomics and Radiogenomics in Neuro-oncology; Shenzhen, China; 2019. pp. 53-60.*
- [28] Nalawade S, Yu FF, Bangalore YCG, Murugesan GK, Shah BR et al. Brain Tumor IDH, 1p/19q, and MGMT molecular classification using MRI-based deep learning: effect of motion and motion correction. *bioRxiv* 2020. doi: 10.1101/2020.06.01.126375
- [29] Pasquini L, Napolitano A, Tagliente E, Dellepiane F, Lucignani M et al. Deep learning can differentiate IDH-mutant from IDH-wild type GBM. *Journal of Personalized Medicine* 2021; 11 (4): 290. doi: 10.3390/jpm11040290
- [30] Fukuma R, Yanagisawa T, Kinoshita M et al. Prediction of IDH and TERT promoter mutations in low-grade glioma from magnetic resonance images using a convolutional neural network. *Scientific Reports* 2019; 9: 20311. doi:10.1038/s41598-019-56767-3
- [31] Decuyper M, Bonte S, Deblaere K, Van HR. Automated MRI based pipeline for segmentation and prediction of grade, IDH mutation and 1p19q co-deletion in glioma. *Computerized Medical Imaging and Graphics* 2021; 88: 101831. doi: 10.1016/j.compmedimag.2020.101831
- [32] Gore S, Chougule T, Jagtap J, Saini J, Ingalthalika M. A review of radiomics and deep predictive modeling in glioma characterization. *Academic Radiology* 2020. doi: 10.1016/j.acra.2020.06.016
- [33] Kessler J, Hohmann T, Güttler A, Petrenko M, Ostheimer C et al. Radiosensitization and a less aggressive phenotype of human malignant glioma cells expressing isocitrate dehydrogenase 1 (IDH1) mutant protein: dissecting the mechanisms. *Cancers (Basel)* 2019; 11(6): 889. doi: 10.3390/cancers11060889
- [34] Houillier C, Wang X, Kaloshi G, Mokhtari K, Guillevin R et al. IDH1 or IDH2 mutations predict longer survival and response to temozolomide in low-grade gliomas. *Journal of Neurology* 2010; 75: 1560-1566.

- [35] Han W, Qin L, Bay C, Chen X, Yu KH et al. Deep transfer learning and radiomics feature prediction of survival of patients with high-grade gliomas. *AJNR American Journal of Neuroradiology* 2020; 41 (1): 40-48.
- [36] Calabrese E, Villanueva-Meyer JE, Cha S. A fully automated artificial intelligence method for non-invasive, imaging-based identification of genetic alterations in glioblastomas. *Scientific Reports* 2020; 10 (1): 11852. doi: 10.1038/s41598-020-68857-8
- [37] Clark K, Vendt B, Smith K, Freymann J, Kirby J et al. The Cancer Imaging Archive (TCIA): maintaining and operating a public information repository. *Journal of Digit Imaging* 2013; 26 (6): 1045–1057. doi: 10.1007/s10278-013-9622-7
- [38] Ceccarelli M, Barthel FP, Malta TM, Sabedot TS, Salama SR et al. Molecular profiling reveals biologically discrete subsets and pathways of progression in diffuse glioma. *Cell* 2016; 164 (3): 550-563.
- [39] Tustison NJ, Avants BB, Cook PA, Zheng Y, Egan A et al. N4ITK: improved N3 bias correction. *IEEE Transaction on Medical Imaging* 2010; 29 (6): 1310-1320.
- [40] Tustison NJ, Cook PA, Klein A, Song G, Das SR et al. Large-scale evaluation of ANTs and FreeSurfer cortical thickness measurements. *Neuroimage* 2014; 99: 166-179.

### Supplementary data: results on different datasets

The proposed 3-pathway method is experimented on three different datasets using the same configuration for each hyperparameter and other parameter (such as batch size, number of epochs, optimizer, loss, network design parameters). The public datasets<sup>1</sup> for machine learning are used to experiment the working of 3-pathway CNN model in order to analyse its effectiveness and impact. The details of datasets are provided below.

1. Brain tumor MRI images: This dataset contains total 3264 gray scale images of random shapes, which were resized to  $200 \times 200$  dimensions and it is used to categorize into four classes i.e. glioma, meningioma, pituitary tumor and no-tumor class.<sup>2</sup>
2. Covid-19 Lungs CT scan data: It consists of total 746 gray scale images of random shapes, which were resized to  $200 \times 200$  dimensions and it is used to categorize into two classes, namely Covid-19 and non-Covid-19 class.<sup>3</sup>
3. Breast histology images: This dataset consists of 5547 breast histology images of size  $50 \times 50 \times 3$ , and it is used to classify as cancerous / IDC images (IDC: invasive ductal carcinoma) vs. non-IDC images.<sup>4</sup>

The results are tabulated in Table S1, which are obtained on the abovementioned datasets using our proposed 3-pathway CNN model.

**Table S1:** Results (accuracy and cross-entropy loss) on different datasets using 3-pathway CNN.

Dataset	Training accuracy (%)	Training loss	validation accuracy(%)	Validation loss	Testing accuracy (%)	Testing loss
Brain tumor MRI	1.0	0.007	91.11	0.494	70.81	5.429
Covid-19 lung data	99.32	0.033	63.08	1.26	72.48	1.160
Breast histology	80.37	0.437	77.92	0.468	78.19	0.470

The graphs of accuracy and cross-entropy loss, obtained during training and validation phases of proposed model and obtained for abovementioned datasets, are shown in Figures S1 and S2.

Table S2 shows the results measured on above mentioned three datasets for three most recent codes<sup>1</sup>.

It can be observed from above two tables that the results of proposed model are comparatively better than almost all abovementioned CNN based models. The first dataset on brain tumor is for 4-class classification and second, third dataset on Covid-19, breast histology is meant for binary classification. In comparison, our 3-pathway model worked better for binary classification for Covid-19 analysis and breast histology analysis. The network design and hyperparameter settings are different in every model of above table. It shows that the proposed 3-pathway model is more effective than the existing methods, which are presented for analysis of different applications like multiclass classification of brain MRI, Covid-19 analysis of lung CT scans, binary classification of histology images for breast cancer detection.

<sup>1</sup>The public datasets available on Kaggle.com.

<sup>2</sup><https://www.kaggle.com/sartajbhuvaji/brain-tumor-classification-mri>

<sup>3</sup><https://www.kaggle.com/luisblanche/covidct>

<sup>4</sup><https://www.kaggle.com/simjeg/lymphoma-subtype-classification-fl-vs-cll>

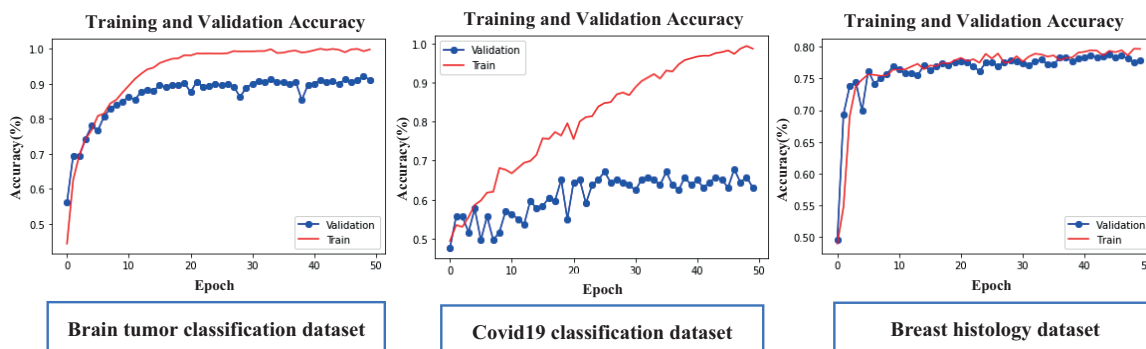


**Figure S1:** Accuracy graph of training and validation phase of 3-pathway CNN model obtained on three different datasets. The number of epochs is shown on x-axis and accuracy is shown on y-axis.

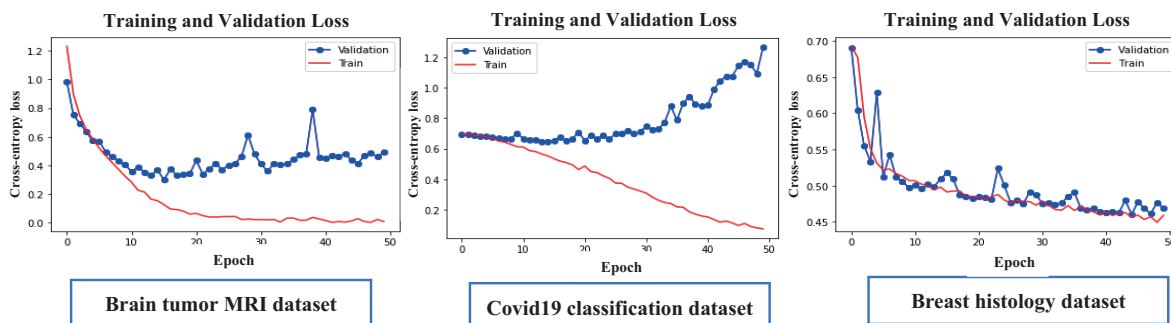


**Figure S2:** Cross-entropy loss graph of training and validation phase of 3-pathway CNN model obtained on three different datasets. The number of epochs is shown on x-axis and cross-entropy loss value is shown on y-axis.



**Table S2:** Results on different datasets for three most recent codes.

Dataset	Details of three recent codes (CNN based models)	Testing accuracy (%)	Testing loss
Brain tumor MRI	Recent code 1 using pretrained VGG16 model <sup>5</sup>	78	In range of 0.1 to 1 (approx.)
Brain tumor MRI	Recent code 2 using pretrained VGG19 model <sup>6</sup>	31	–
Brain tumor MRI	Recent code 3 using pretrained ImageNet model <sup>7</sup>	95	–
Covid-19 lung CT scan	Recent code 1 <sup>8</sup>	53.38	166.8
Covid-19 lung CT scan	Recent code 2 <sup>9</sup>	66.21	0.563
Covid-19 lung CT scan	Recent code 3 <sup>10</sup>	70.58	2.874
Breast histology	Recent code 1 <sup>11</sup>	77.12	0.491
Breast histology	Recent code 2 <sup>12</sup>	In range of 50.34 to 73.80	In range of 0.934 to 0.552
Breast histology	Recent code 3 <sup>13</sup>	73.87	0.505

<sup>5</sup><https://www.kaggle.com/abhijitsingh001/braintumor-classification-cnn-vs-transferlearning><sup>6</sup><https://www.kaggle.com/rohandeysarkar/tumor-classification><sup>7</sup><https://www.kaggle.com/jaykumar1607/brain-tumor-mri-classification-tensorflow-cnn><sup>8</sup><https://www.kaggle.com/sakshamkumarsharma/workof><sup>9</sup><https://www.kaggle.com/barnadeepdey/covid-ct-prediction><sup>10</sup><https://www.kaggle.com/vipulshahi/image-data-for-lungs><sup>11</sup><https://www.kaggle.com/anubhovmenon/breast-cancer><sup>12</sup><https://www.kaggle.com/burakkahveci/image-classification-with-ml-algorithms-dl-alg#Transfer-Learning-Section-VGG19-><sup>13</sup><https://www.kaggle.com/abhisheksss/cancer-images-detection>